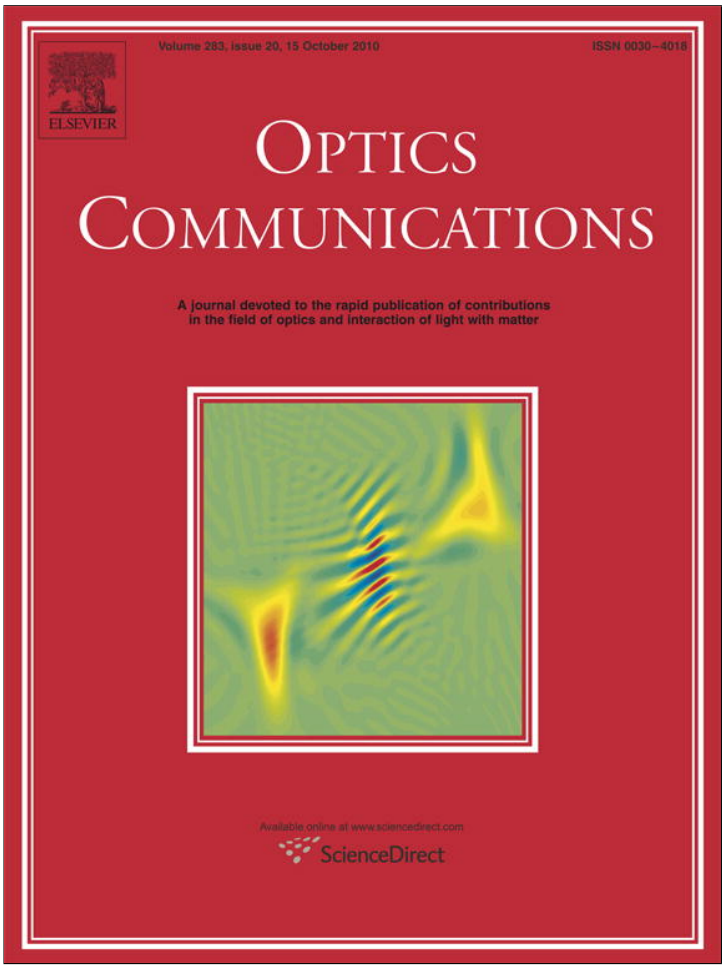

Optics Communications 283 (2010) 4074–4077

Contents lists available at ScienceDirect

Optics Communications

journal homepage: www.elsevier.com/locate/optcom

Effective optical parameters of thin-film and bulk metamaterials of metallodielectric nanosandwiches

C. Tserkezis [a,*], N. Stefanou [a], N. Papanikolaou [b]

[a] Section of Solid State Physics, University of Athens, Panepistimioupolis, GR-157 84 Athens, Greece
[b] Institute of Microelectronics, NCSR "Demokritos,"GR-153 10 Athens, Greece

ARTICLE INFO

Article history:
Received 21 December 2009
Received in revised form 15 April 2010
Accepted 25 May 2010

Keywords:
Metallodielectric nanosandwich
Effective constitutive parameters
Optical magnetism
Multiple scattering
Photonic band structure

ABSTRACT

We report on the effective optical response of single- and multilayer periodic structures of metallodielectric nanosandwiches on the basis of rigorous, full-electrodynamic calculations by the extended layer-multiple-scattering method. It is shown that the complex photonic band structure and the reflection coefficient of the infinite and semi-infinite crystal, respectively, provide reliable bulk effective parameters, which can be used as a reference in order to resolve ambiguities and problems in the determination of these parameters for finite slabs by the *S*-matrix retrieval procedure. Our results show that the structures under consideration exhibit strong artificial optical magnetism and thin films consisting of a few layers already behave like the bulk metamaterial.

1. Introduction

Among the various plasmonic structures, metal–dielectric-metal nanosandwiches, made of a pair of in-tandem metallic nanodisks separated by a dielectric spacer, have attracted considerable interest in recent years because of their unique optical properties [1–7]. Particle plasmons of the two metallic disks interact with each other, giving rise to two hybridized plasmonic modes; the one at higher frequency is symmetric and corresponds to a net electric dipole moment, while the lower one is antisymmetric and corresponds to a magnetic dipole moment [3]. It has been demonstrated that in a periodic array of such composite particles the antisymmetric mode can lead to the occurrence of artificial magnetism at near infrared and visible frequencies [7], which renders these structures promising candidates for single- or double-negative metamaterials [8]. Unlike metamaterials based on metallic nanorods [9], split-ring resonators [10], metallic nanowires [11] or cut-wire pairs [12], which operate at a specific polarization mode of the electromagnetic (EM) field, metal–dielectric-metal nanosandwiches, because of their cylindrical symmetry, offer the possibility for designing polarization-insensitive metamaterials. Moreover, it has been shown that the spectral region where the above-mentioned hybridized plasmonic modes appear can be easily tuned by modifying either the lattice constant(s) of the structure [6,7] or the thickness of the dielectric spacer [1].

The problem of assigning effective EM parameters to a heterogeneous medium has recently emerged as an important issue in relation to optical metamaterials and various homogenization methods have been proposed [13–18]. One of the most commonly used methods is the so-called *S*-matrix retrieval procedure [13,14,19], which imposes the scattered wave from a planar slab of the heterogeneous medium in the far-field zone, i.e. the complex transmission and reflection coefficients (*S*-matrix elements), to be the same with that scattered from a slab of a hypothetical homogeneous material. However, this technique often leads to nonphysical material parameters as a result of forcing a homogeneous material to reproduce exactly the features of the wave field scattered by the actual heterogeneous medium [20–22].

In this paper we use the *S*-matrix retrieval procedure to determine the effective permittivity and permeability functions that describe the optical response of single- and multilayer structures of metal–silica–metal nanosandwiches, at normal incidence. We show how problems inherent to this retrieval procedure can be overcome by appealing to the corresponding effective parameters of the bulk metamaterial, deduced from the complex band structure and the reflection coefficient of the infinite and semi-infinite crystal, respectively. Moreover, we study the evolution of the effective parameters with increasing slab thickness and discuss the transition from thin-film to bulk behavior.

2. Model and method of calculation

We consider single- and multilayer structures of metal–silica–metal nanosandwiches, in air. We assume that the optical response of

* Corresponding author. Tel.: +30 210 7276758; fax: +30 210 7276711.
E-mail addresses: ctserk@phys.uoa.gr (C. Tserkezis), nstefan@phys.uoa.gr (N. Stefanou), N.Papanikolaou@imel.demokritos.gr (N. Papanikolaou).

0030-4018/$ – see front matter © 2010 Elsevier B.V. All rights reserved.
doi:10.1016/j.optcom.2010.05.049

the metallic material is described by the Drude relative permittivity function [23]

$$\varepsilon_m = 1 - \frac{\omega_p^2}{\omega(\omega + i\tau^{-1})}, \quad (1)$$

where ω_p is the bulk plasma frequency and τ the relaxation time of the conduction-band electrons that accounts for dissipative losses, and a relative permeability $\mu_m = 1$. For silica, we take $\varepsilon_{silica} = 2.13$ and $\mu_{silica} = 1$. For convenience, we choose to use ω_p as the frequency unit and c/ω_p as the length unit, where c is the velocity of light in vacuum. We note that, considering a typical value 10 eV for $\hbar\omega_p$, c/ω_p corresponds to about 20 nm.

The nanosandwiches under consideration consist of a pair of in-tandem metallic nanodisks of radius $S = 2.5c/\omega_p$ and equal thickness $h_1 = h_3 = c/\omega_p$, separated by a silica spacer of thickness $h_2 = 2c/\omega_p$. Therefore, $h = h_1 + h_2 + h_3 = 4c/\omega_p$ is the total thickness of the nanosandwich. In each layer, the nanosandwiches are arranged on a hexagonal lattice defined by the primitive vectors $\mathbf{a}_1 = a_0(1, 0, 0)$ and $\mathbf{a}_2 = a_0(1/2, \sqrt{3}/2, 0)$, with $a_0 = 10c/\omega_p$, while consecutive layers are displaced by $\mathbf{a}_3 = (a_0/2, a_0\sqrt{3}/6, h)$, so that the distance between them is $d = h$. A schematic view of the structure is shown in Fig. 1.

We employ the extended layer-multiple-scattering method [24–26], which is ideally suited for the structure under consideration, to carry out full-electrodynamic band structure and reflection/transmission calculations. Besides the complex photonic band structure of the infinite crystal, the method allows one to calculate, also, the reflection and transmission coefficients of an EM wave incident at any angle on a finite slab or on the semi-infinite crystal [27] and, in this respect, it can describe an actual transmission experiment. Another advantage of the method is that it proceeds at a given frequency, i.e., it is an on-shell method and, therefore, it can treat strongly dispersive materials such as metals and include losses, which always exist in real materials, in a straightforward manner. The properties of the individual scatterers enter only through the corresponding T matrix which, for homogeneous spherical particles, is given by the closed-form solutions of the Mie-scattering problem, while for scatterers of arbitrary shape it is calculated numerically by the extended-boundary-condition method [28]. At a first step, in-plane multiple scattering is evaluated in a spherical-wave basis using proper propagator functions. Subsequently, interlayer scattering is calculated in a plane-wave basis through appropriate reflection and transmission matrices. The scattering S-matrix of a multilayer slab, which transforms the incident into the outgoing wave field, is obtained by combining the reflection and transmission matrices of the component layers. The ratio of the transmitted or reflected energy flux to the energy flux associated with the incident wave defines the transmittance or reflectance of the slab, respectively.

In order to ensure adequate convergence in our calculations for the structures under consideration, we truncate the spherical-wave expansions at $\ell_{max} = 14$ and take into account 61 two-dimensional reciprocal lattice vectors in the relevant plane-wave expansions, while the single-particle scattering T matrix is evaluated with $\ell_{cut} = 20$ and a Gaussian quadrature integration formula with 6000 points [26].

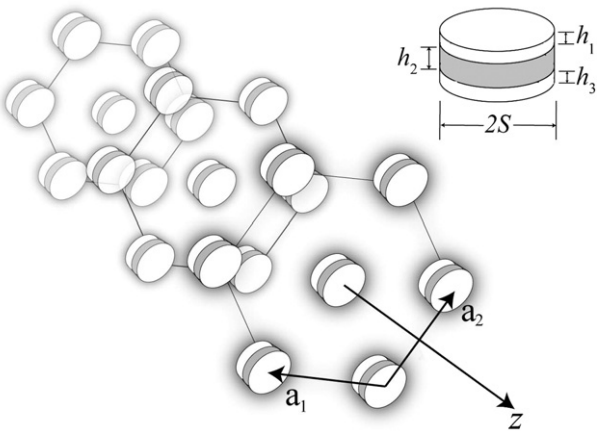

Fig. 1. Schematic view of the layered structure of metal–silica–metal nanosandwiches under consideration.

3. Results and discussion

The complex photonic band structure of the crystal under consideration if we neglect dissipative losses ($\tau^{-1} = 0$ in Eq. (1)) along the growth direction, up to and including the frequency region of the antisymmetric mode that interests us here, is displayed in Fig. 2. At low frequencies we obtain a doubly degenerate linear dispersion line, as expected for propagation in a homogeneous medium characterized by a frequency-independent refractive index. This band interacts with the narrow doubly degenerate band which originates from the antisymmetric modes of the individual nanosandwiches and, as a result, a hybridization gap opens up about the crossing point. In the gap region there are no propagating modes of the EM field and the dispersion lines continue analytically in the complex k_z plane [29]. Over this region we show the dispersion lines for complex values of k_z that correspond to the doubly degenerate bands with the smallest in magnitude imaginary part and, therefore, they are the ones which determine light propagation in the crystal along the given direction. Such complex bands have been studied by a number of authors in relation to the electron band structure of crystalline solids (see, e.g., Ref. [30]) and have been proven to satisfy some interesting theorems, which also apply to photonic bands. If we take into account dissipative losses in the metallic material assuming a finite value for the relaxation time in Eq. (1), even the real bands acquire a small imaginary part and move into the complex k_z plane.

Next to the band diagram in Fig. 2, we show the reflectance at normal incidence of a finite slab of the above crystal consisting of eight layers of nanosandwiches, together with that of the corresponding semi-infinite crystal. The reflectance of the finite slab exhibits the well-known Fabry–Perot oscillations, which are due to multiple reflections between the surfaces of the slab. These oscillations appear

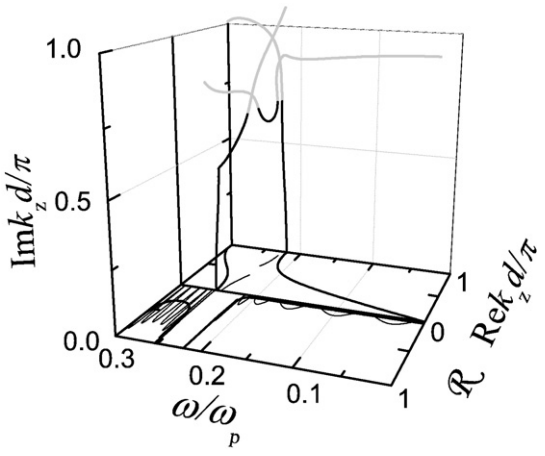

Fig. 2. The complex photonic band structure of the crystal under consideration along the [001] direction, neglecting absorptive losses. The segments of the (doubly degenerate) complex bands with the smallest in magnitude imaginary part over the gap region are shown by thick black lines. The thin lines show the projection of these bands on the $\omega - \mathrm{Re}k_z$ plane. Next to the band diagram we display the reflectance at normal incidence of a slab of eight (001) planes of the crystal (thin line) together with the reflectance of the corresponding semi-infinite crystal (thick line).

both below and above the gap, and their period corresponds to $k_z d/\pi = 1/8$, as expected for the given thickness. On the contrary, the reflectance of the semi-infinite crystal does not exhibit such oscillations, because there is no rear surface in this case. In the frequency region of the gap, since there are no propagating modes of the EM field, the transmittance goes to zero, and, therefore, the reflectance becomes unity.

We shall now try to assign to the crystal under consideration effective permittivity and permeability functions, appropriate to normally incident light. Clearly, here, an effective-medium description is applicable because the free-space wavelength is much larger than the size of the particles and the distances between them ($20c/\omega_p \lessapprox \lambda < \infty$) and, moreover, there is a single dominant relevant Bloch mode at any frequency (see Fig. 2). Since the distance, d, between consecutive lattice planes normal to the growth direction is equal to the total thickness, h, of the nanosandwich ($=4c/\omega_p$), we assume this also to be the effective layer thickness. Therefore, the total thickness of a slab consisting of N_L layers of nanosandwiches is $4N_L c/\omega_p$. We calculate the effective parameters of a slab of the given crystal using the so-called S-matrix retrieval procedure, which is based on the inversion of Fresnel's equations for a set of transmission and reflection coefficients, t and r, respectively (S-matrix parameters). The calculated t and r for finite slabs of the crystal under consideration, one-, two- and eight-layers thick, at normal incidence, are displayed in Fig. 3. However, the S-matrix retrieval method encounters some problems. For example, as discussed in Ref. [13], the calculation of the effective refractive index requires solving an equation which involves a multivalued function (the arctan function). When dealing with a single layer of a metamaterial, it is usually the fundamental branch that is relevant. For relatively thick slabs, however, the branches may lie very close to each other, making the selection of the correct branch a rather difficult task. In addition, possible discontinuities due to resonances complicate further the determination of an effective refractive index. This problem can be overcome by using as a reference the effective refractive index deduced from the complex band structure of the corresponding infinite crystal, $n_{eff} = c[Rek_z + iImk_z]/\omega$, which is calculated in an unambiguous manner. Interestingly, in the gap region, Ren_{eff} varies stairwise and corresponding peaks appear in Imn_{eff}, as many as the number of layers of the slab. These structures, also observed by others [31], are associated with in-gap resonances of the slab [29,32]. As more layers are stacked together to build the infinite crystal, these structures come closer to each other and become less sharp, leading to the smooth refractive index deduced from the corresponding complex band structure of the infinite crystal. It is worth noting that, in the presence of absorption, these features are further smoothed out.

On the other hand, calculation of the effective impedance, z_{eff}, of the slabs under consideration shows the existence of spurious sharp structures at the Fabry-Perot resonances. Such structures have been found by others as well and were attributed to the thickness of the slab [31] and more specifically to Fabry–Perot resonances [33], but only recently a detailed and rigorous analysis of their origin was presented [32]. In order to get rid of these artifacts, we can appeal to the effective impedance of the corresponding semi-infinite crystal, which is readily obtained from the associated complex reflection coefficient, r_∞, through the equation $z_{eff} = z_{env}(1+r_\infty)/(1-r_\infty)$, where z_{env} is the impedance of the environment. Obviously, z_{eff} does not exhibit the above-mentioned spurious structures because there is no rear surface to generate multiple reflections that cause the Fabry–Perot resonances.

In Fig. 4 we display the effective permittivity, ε_{eff}, and permeability, μ_{eff}, deduced from z_{eff} and n_{eff} ($\varepsilon_{eff} = n_{eff}/z_{eff}$ and $\mu_{eff} = n_{eff} z_{eff}$), as obtained by the S-matrix procedure for slabs one-, two- and eight-layers thick, together with the corresponding parameters obtained for the bulk metamaterial as described here above, in the presence of absorptive losses ($\tau^{-1} = 0.025\omega_p$). We can clearly see a strong resonance in the effective permeability, which is the fingerprint of artificial optical magnetism, accompanied by a relatively weak antiresonance in the effective permittivity, an effect which is discussed by others as well [19,20,31,34]. Interestingly, the effective parameters converge very fast with increasing slab thickness. Already a bilayer behaves much like the bulk metamaterial, while $\varepsilon_{eff}(\omega)$ and $\mu_{eff}(\omega)$ for the eight-layers thick slab are practically identical to their counterparts for the infinite crystal. Finally, it is worth noting that the retrieved effective parameters are independent of the polarization of the (normally) incident wave, as expected from the symmetry of the structure.

4. Conclusion

In summary, we evaluated the effective permittivity and permeability functions that describe the optical response at normal incidence of thin-film and bulk hexagonal structures of metal–silica–metal nanosandwiches, in the presence of absorption, by means of full-electrodynamic calculations using the extended layer-multiple-scattering method. Employing the S-matrix retrieval procedure for finite slabs, in conjunction with corresponding bulk results obtained from complex band structure

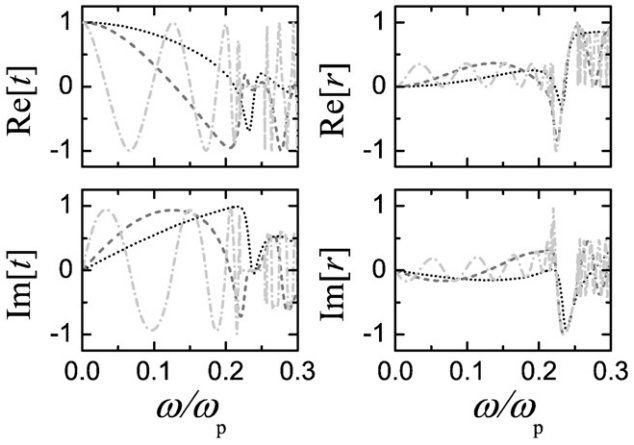

Fig. 3. Complex S-matrix parameters of one- (dotted lines), two- (dashed lines) and eight- (dash-dotted lines) layers thick (001) slabs of the crystal under consideration (neglecting absorptive losses), at normal incidence.

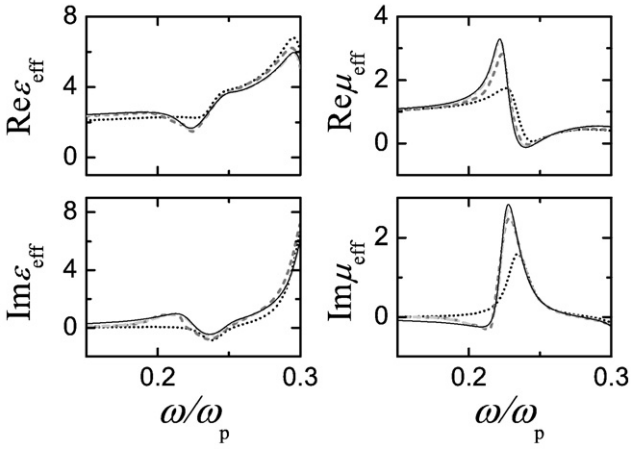

Fig. 4. The real (upper diagrams) and imaginary (lower diagrams) parts of the effective permittivity (left-hand panel) and permeability (right-hand panel) functions deduced for one- (dotted lines), two- (dashed lines) and eight- (dash-dotted lines) layers thick (001) slabs of the crystal under consideration including absorptive losses ($\tau^{-1} = 0.025\omega_p$), at normal incidence. The solid lines show the corresponding results for the bulk metamaterial, which are indiscernible from those of the eight-layer slab.

and reflection-coefficient calculations, we can study the transition from thin-film to bulk behavior of the given metamaterial and, at the same time, resolve ambiguities and problems inherent to the *S*-matrix method. Our results reveal the occurrence of strong artificial optical magnetism and a fast convergence to the bulk response with increasing slab thickness.

Acknowledgement

This work was supported by the research programme "Kapodistrias" of the University of Athens.

References

[1] K.H. Su, Q.H. Wei, X. Zhang, Appl. Phys. Lett. 88 (2006) 063118.
[2] K.H. Su, S. Durant, J.M. Steele, Y. Xiong, C. Sun, X. Zhang, J. Phys. Chem. B 110 (2006) 3964.
[3] T. Pakizeh, M.S. Abrishamian, N. Granpayeh, A. Dmitriev, M. Käll, Opt. Express 14 (2006) 8240.
[4] A. Dmitriev, T. Pakizeh, M. Käll, D.S. Sutherland, Small 3 (2007) 294.
[5] S.M. Wang, T. Li, H. Liu, F.M. Wang, S.N. Zhu, X. Zhang, Opt. Express 16 (2008) 3560.
[6] Y. Ekinci, A. Christ, M. Agio, O.J.F. Martin, H.H. Solak, J.F. Löffler, Opt. Express 16 (2008) 13287.
[7] C. Tserkezis, N. Papanikolaou, G. Gantzounis, N. Stefanou, Phys. Rev. B 78 (2008) 165114.
[8] N. Feth, C. Enkrich, M. Wegener, S. Linden, Opt. Express 15 (2007) 501.
[9] V.M. Shalaev, W. Cai, U.K. Chettiar, H.-K. Yuan, A.K. Sarychev, V.P. Drachev, A.V. Kildishev, Opt. Lett. 30 (2005) 3356.
[10] C. Rockstuhl, T. Paul, F. Lederer, T. Pertsch, T. Zentgraf, T.P. Meyrath, H. Giessen, Phys. Rev. B 77 (2008) 035126.
[11] W. Park, Q. Wu, Solid State Commun. 146 (2008) 221.
[12] B. Kanté, S.N. Burokur, A. Sellier, A. de Lustrac, J.-M. Lourtioz, Phys. Rev. B 79 (2009) 075121.
[13] D.R. Smith, S. Schultz, P. Markoš, C.M. Soukoulis, Phys. Rev. B 65 (2002) 195104.
[14] X. Chen, T.M. Grzegorcyk, B.-I. Wu, J. Pacheco Jr., J.A. Kong, Phys. Rev. E 70 (2004) 016608.
[15] J.-M. Lerat, N. Malléjac, O. Acher, J. Appl. Phys. 100 (2006) 084908.
[16] M.G. Silveirinha, Phys. Rev. B 75 (2007) 115104.
[17] C.R. Simovski, S.A. Tretyakov, Phys. Rev. B 75 (2007) 195111.
[18] A.I. Căbuz, D. Felbacq, D. Cassagne, Phys. Rev. Lett. 98 (2007) 037403.
[19] D.R. Smith, D.C. Vier, Th. Koschny, C.M. Soukoulis, Phys. Rev. E 71 (2005) 036617.
[20] T. Koschny, P. Markoš, D.R. Smith, C.M. Soukoulis, Phys. Rev. E 68 (2003) 065602 (R).
[21] R.A. Depine, A. Lahtakia, Phys. Rev. E 70 (2004) 048601.
[22] A.L. Efros, Phys. Rev. E 70 (2004) 048602.
[23] N.W. Ashcroft, N.D. Mermin, Solid State Physics, Saunders, New York, 1976.
[24] N. Stefanou, V. Yannopapas, A. Modinos, Comput. Phys. Commun. 113 (1998) 49.
[25] N. Stefanou, V. Yannopapas, A. Modinos, Comput. Phys. Commun. 132 (2000) 189.
[26] G. Gantzounis, N. Stefanou, Phys. Rev. B 73 (2006) 035115.
[27] C. Tserkezis, N. Stefanou, Phys. Rev. B 81 (2010) 115112.
[28] M.I. Mishchenko, L.D. Travis, A.A. Lacis, Scattering, Absorption, and Emission of Light by Small Particles, Cambridge University Press, Cambridge, 2002.
[29] G. Gantzounis, N. Stefanou, Phys. Rev. B 72 (2005) 075107.
[30] V. Heine, Proc. Phys. Soc. London 81 (1963) 300.
[31] T. Koschny, P. Markoš, E.N. Economou, D.R. Smith, D.C. Vier, C.M. Soukoulis, Phys. Rev. B 71 (2005) 245105.
[32] C. Tserkezis, J. Phys. Condens. Matter 21 (2009) 155404.
[33] A. Andryieuski, R. Malureanu, A.V. Lavrinenko, Phys. Rev. B 80 (2009) 193101.
[34] S. O' Brien, J.B. Pendry, J. Phys. Condens. Matter 14 (2002) 4035.